

## An operational coastal forecasting tool for performing ensemble modeling

Peyman Taeb\*, Robert J. Weaver

Department of Ocean Engineering and Sciences, 150 W. University Blvd., Florida Institute of Technology, Melbourne, FL, 32901, USA



### ARTICLE INFO

**Keywords:**

ADCIRC  
One-way nesting  
Coastal forecasting software  
Ensemble modeling  
Efficiency

### ABSTRACT

An automated coastal estuarine modeling system, termed *Multistage*, is created in the ADCIRC hydrodynamic model. The software development was motivated by the need for reducing the simulation wall-clock time to increase the scalability of ADCIRC for *ensemble modeling*. *Multistage* makes use of a one-way nesting technique as an alternative to the continuous single-domain approach. Hydrodynamic predictions, such as storm surge and waves, are made for a targeted coastal region in a two-stage scheme consisting of a large-scale coarse mesh simulation and a small-scale fine mesh simulation. The nesting technique is adjusted for accurate and efficient coastal estuarine modeling with careful considerations. We propose and successfully test a method for the coarse mesh extending onshore rather than the common practice of extending the fine mesh offshore. Repetitive ensemble computations are allowed over both the coarse mesh and the fine mesh in an efficient time frame. Modeling preparations and processes are scripted to eliminate the additional efforts needed for applying this model nesting technique. The tool is tested on two coastal estuarine systems, and its performance is compared with the conventional single-domain method and observational data. By implementing *Multistage*, forecast runtimes are reduced by 50% to more than 80% using the same model parameters and computational resources as used in the conventional single-domain technique. Depending on the domain and model type, it is possible to perform 3-to-5 ensemble simulations on both coarse and fine meshes by applying the nesting technique and using the same amount of CPU-hours needed to complete one single-domain simulation. This research details the concept, preliminary results and offline applications of the tool. Future work is focused on enhancing the ease of use and on development and implementation of a real-time version.

### 1. Introduction

Numerical modeling of coastal circulation and waves has evolved considerably over the past few decades, as a result of rapid improvements in computing power (speed, memory, etc.) and scientific knowledge (Hinkelmann, 2006; Tezduyar et al., 1996). The increase in computing capacity has encouraged modelers to create domains with large regions of high resolution. This increased resolution has, in turn, provided a more realistic representation of coastal flows. While access to High-Performance Computing, HPC, resources continue to improve, full-scale hydrodynamic simulations are expensive, and large ensemble forecasts are still not possible in real time. In the absence of increased computing resources, an optimization such as a new modeling approach or numerical technique is necessary. The goal of this research is to reduce the computational cost of high-resolution hydrodynamic modeling with the ADvanced CIRCulation (ADCIRC) model. An automated modeling system, designed for modeling coastal estuarine systems referred to as “*Multistage*,” is created and applied in the ADCIRC model framework. Like its parent system, the *Multistage* tool can incorporate

atmospheric, wind-wave, and land use models to account for a variety of applications – but with the addition of an automated coupling tool. State-of-the-art conventional one-way (C1W) nesting, comprising a (large-scale) coarse mesh and (small-scale) fine mesh, is applied with careful considerations and adjustments to maintain model accuracy.

In C1W nesting, a coarse-resolution outer model communicates to a fine-resolution inner model through the specification of the open boundary conditions of the fine-resolution model. The main disadvantage is that the fine-resolution grid does not communicate to the coarse-resolution grid, so the inner model does not update the solutions on the coarse grid. Inter-grid communication can be two-way as suggested by Oey and Chen (1992). In two-way nesting, the coarse grid outer model variables are continually replaced by inner model variables where the two grids overlap so that the outer model benefits from the fine resolution of the inner model through the grids interface (Harris and Durrant, 2010; Sheng et al., 2005). This paper describes the implementation of C1W nesting in the ADCIRC model. Since the coarse-resolution and fine-resolution models are run sequentially in C1W nesting, it is computationally efficient and is preferred over two-way

\* Corresponding author.

E-mail addresses: [ptae2014@my.fit.edu](mailto:ptae2014@my.fit.edu) (P. Taeb), [rjweaver@fit.edu](mailto:rjweaver@fit.edu) (R.J. Weaver).

nesting. In addition to taking advantage of the efficiency associated with C1W nesting, *Multistage* also accounts, in part, for the impact of the coastal estuary on the coastal ocean by extending the coarse mesh onshore.

*Multistage* is the first automated system developed for nesting applications within the ADCIRC community. Automation is beneficial as it eliminates the burden associated with mesh preparation, boundary forcing processing, and model setup. The tool reads model parameters from a configuration file and carries out all processing automatically via bash, Perl, and FORTRAN scripts. *Multistage* is licensed as an open source software<sup>1</sup> and is available to the community. Preliminary applications of *Multistage* indicates an approximately 50% to more than 80% wall-clock time reduction compared to conventional single-domain techniques with ADCIRC (Taeb and Weaver, 2017).

In the past few decades, there have been several efforts on coupling models and nesting grids in coastal and ocean modeling communities (e.g., Blain et al., 2009; Ji et al., 2010; Qi et al., 2018; Zheng and Weisberg, 2012). Within most of them, a high-resolution shallow water model representing complex irregular coastal dynamics is nested to a regional or global ocean model that represents the circulation patterns of larger-scale flows. The model representing larger-scales does not have to be the same as the finer-scale model. Depending on physical processes and domain characteristics of study, structured-grid or unstructured-mesh nesting techniques are applied.

Blain et al. (2009), for example, studied the density-driven two-layer flow in the Dardanelles strait by nesting ADCIRC and the structured-grid Hybrid Coordinate Ocean Model (HYCOM) (HYCOM: Chassignet et al., 2007; Halliwell et al., 2000). In their study, ADCIRC is applied to provide the resolution necessary to represent the flow in the narrow complex strait, obtaining the initial and boundary conditions from HYCOM. Another instance of nesting ADCIRC to HYCOM is within the Real-Time Operational Forecast System (RTOFS). RTOFS is run at the National Center for Environmental Prediction (NCEP) for the Atlantic basin and is based on the HYCOM model. The RTOFS output is provided as initial and boundary conditions to the ADCIRC model which is configured for specific domains on the east coast of the US employing high-resolution unstructured meshes (Ji et al., 2010). Zheng and Weisberg (2012) studied the density-driven oceanic and coastal circulation in three-dimensions for the West Florida Continental Shelf (WFS) for the calendar year 2007. The study was conducted by nesting a coastal region model, the unstructured Finite-Volume Coastal Ocean Model (FVCOM), with the structured-grid global HYCOM. FVCOM resolves the material properties exchange between separate estuaries along the west coast of Florida and also the interaction between estuaries and the continental shelf. Qi et al. (2018) developed a module of FVCOM under the standard Earth System Modeling Framework (ESMF). ESMF-FVCOM applies an unstructured-to-unstructured mesh nesting technique and supports both one-way and two-way nesting approaches. The regional FVCOM with the computational domain covering the Gulf of Maine, Georges Bank, and New England Shelf region (GOM-FVCOM) was nested to the Mass Coastal FVCOM resolving detailed coastal features.

The advantages of the unstructured-mesh nesting are its simple implementation and better performance in retaining the consistency and continuity of computed variables at the interface of two nested domains compared to structured-grid nesting (Qi et al., 2018). Modeling coastal and estuarine flows with a structured grid will usually require multiple layers of nesting to achieve the high resolution needed at the coastal level while optimizing the mesh in the deep open ocean. An unstructured mesh typically can eliminate the need for multiple layers of nesting because the mesh will vary in resolution, moving from coarse deep ocean to a fine-scale resolution in complex and irregular coastal and inter-coastal regions (Zheng and Weisberg, 2012).

*Multistage* takes advantage of the variable resolution in an unstructured mesh to optimize the C1W nesting.

The method applied in this study is similar to the subdomain modeling approach (Baugh et al., 2015; Altuntas and Baugh, 2017). Both techniques perform a large domain simulation to obtain boundary conditions which are used to force the boundaries of a local mesh. While making use of the similar approach to reduce computational effort, *Multistage* and Subdomain modeling are different regarding application and implementation. *Multistage* is developed for modeling surface circulation and waves in coastal oceans and coastal estuaries, especially for short-term meteorological events such as tropical storm, hurricanes, and frontal passages. Subdomain modeling is a reanalysis technique for assessing local modifications of a grid and iterative design scenarios in that parameters of a limited geographical region are required to be re-calculated. Subdomain Modeling performs a one-time, large-scale simulation to produce boundary conditions for subsequent re-computations on a target subdomain with local changes. In contrast, *Multistage* performs simulations for each scenario associated with altered storm parameters on both the large-scale and the limited region of study within a reasonable time frame.

While a local mesh is a sub-grid in Subdomain Modeling, the fine mesh, in *Multistage*, is not a sub-grid of the larger-scale mesh. This strategy allows for configuration of a coarse mesh with significantly coarser-resolution. The use of the latest versions of Subdomain Modeling necessitates the development of a new software architecture for ADCIRC; however, any version of ADCIRC can be adapted in the *Multistage* nesting application. The current version of the *Multistage* tool supports only specified elevation boundary condition while Subdomain Modeling makes use of a more representative type of boundary conditions (combined water surface elevation, wet/dry status, and current velocity at the interface of full-domain and sub-domain meshes). Neither method currently includes wave information along the boundaries as a component of the boundary conditions (Altuntas and Baugh, 2017; Baugh et al., 2015).

## 2. Background

### 2.1. Hydrodynamics: circulation model

The ADvanced CIRCulation (ADCIRC) model (Luettich et al., 1992; Luettich and Westerink, 2015) is a software package commonly used by the Federal Emergency Management Agency (FEMA), the U.S. Army Corps of Engineers (USACE), academic research groups, and local agencies. The system computes sea surface elevations and currents due to mesoscale processes such as tides and meteorological conditions (e.g., hurricanes). The model applies the continuous-Galerkin, finite-element (FE) method by using a  $C^0$  interpolating basis function with linear two-dimensional triangular elements in space, and the finite difference (FD) method in time. Such an unstructured-mesh model is required for high-resolution coastal ocean circulation modeling. ADCIRC solves the Generalized Wave Continuity Equation (GWCE) to compute the surface elevation, and a modified form of the shallow-water equation to compute the current velocity on an unstructured mesh. Using the GWCE eliminates the spurious oscillation mode problems caused by early shallow-water equations leading to the development of a robust FE depth-integrated coastal circulation model such as the ADCIRC model (Luettich et al., 1992; Luettich and Westerink, 2006; Lynch and Gray, 1979; Walters and Carey, 1983).

### 2.2. Hydrodynamics: coupled circulation and wave model

ADCIRC is typically coupled with a wave model to provide wave forecast/hindcast along with a more accurate prediction of surface elevation and current velocity. Although circulation is a separate physical process from wind-waves, waves are affected by the circulation and vice-versa. Wind-induced waves contribute to water level rise by

<sup>1</sup> <https://github.com/ptaeb2014/Multi-stage>.

10–15% in storm tides, 5–20% on continental shelves, and 30% on steep slope regions (Dietrich et al., 2011; Weaver and Slinn, 2005). This change in water levels will affect wave breaking and propagation. On the other hand, waves can affect water level and currents through wave momentum flux. Wind-waves can also increase the surface roughness and vertical mixing momentum and change the bottom friction which in turn impacts circulation (Bunya et al., 2010; Dietrich et al., 2011; Funakoshi et al., 2008; Roland et al., 2012; Weaver and Slinn, 2005).

To predict wave characteristics, Simulating Waves Nearshore (SWAN), is tightly coupled with ADCIRC (ADCIRC + SWAN) (Dietrich et al., 2012, 2011; Hope et al., 2013). SWAN is a third generation phase-averaged wave model. Compared to WAM (Cycle 3 and 4) and WAVEWATCH III, SWAN contains additional formulations for shallow water so that it is suitable for coastal estuarine modeling. SWAN numerical implementation is implicit and therefore unconditionally stable. It solves the evolution of action density  $N(t, \lambda, \phi, \theta, \sigma)$  over time  $t$  and geographical space ( $\lambda, \phi$ ), and spectral space of direction ( $\theta$ ) and frequency ( $\sigma$ ). Wave properties, such as wave heights and periods, are computed by integrating action density (Booij et al., 2004, 1999).

ADCIRC passes water levels, current velocities, wind velocities, and friction roughness lengths to SWAN where water depth, wave propagation, depth-induced breaking, and other wave processes are calculated. SWAN passes wave information, wave action, the ratio of group velocity to phase velocity, and relative frequency, to the ADCIRC model where radiation stress gradients are calculated at each vertex (Dietrich et al., 2013, 2011). The ADCIRC and SWAN models are tightly coupled, i.e., the coupled model system benefits from utilizing the same unstructured mesh and sharing the same sub-grids in parallel applications.

### 2.3. Conventional scheme: continuous single-domain

In the traditional single domain approach, the model system is run to spin up applied boundary conditions. Surface elevations are spun-up by forcing astronomical tidal constituents on open-ocean boundaries, and if desired, river inflow is spun-up by applying flow rates at specified nodes along river boundaries. The model can also be forced using meteorological forcing, and wave radiation-stress gradient (Dietrich et al., 2011; Funakoshi et al., 2008). Depending on geometry, bathymetry, bottom friction, viscosity, etc. (Stelling et al., 1986), as well as the characteristics of the tidal constituents (Lyard et al., 2006), tidal signals can take a significant amount of time to fully propagate across the domain and reach the condition in which the domain is completely adjusted to boundary forcing, “spun-up”. Due to the effects of tides on currents and surface elevation (Chen et al., 2003), it is necessary to perform a tidal spin-up simulation to accurately create the initial conditions at the beginning of the event simulation. A spin-up run can add a notable amount of time to total forecast. It is also vital to place open ocean boundary far away from immediate coastal regions of study. Westerink et al. (1992) explained two main rationales behind this strategy in their research. First, it is difficult to specify the surface elevations and currents at boundaries of the immediate area of interest. Second, there are flow features that make it desirable to define expanded computational domain beyond the continental shelf adjacent to the area of interest. Hurricane-induced effects at boundaries such as the hurricane forerunner, complex wind patterns associated with a hurricane driving the flow onto the shelf, and resonant shelf edge waves are among flow features that require far field open-ocean boundaries.

For modeling coastal circulation on the U.S. east coast, typical modeled domains cover the West North Atlantic Ocean, Caribbean Sea, and the Gulf of Mexico between 98°W and 60.7°W and between 9°N and 47°N. This type of grid is referred to as “expanded domain with flexible resolution” which places the open boundary far from the area of interest to minimize the boundary effects (Westerink et al., 1992). To study hydrodynamics inside a lagoon, the coastal ocean domain and beyond must be included in the computation. This necessity involves model calculations at a large number of points; whereas, in most cases,

the researcher is only interested in hydrodynamic predictions and measurements within a small portion of the full domain, such as in estuarine modeling.

## 3. Multistage

### 3.1. General description

Implementing one-way nesting is a two-stage scheme, each providing hydrodynamic solutions for separate geographical regions. In the first stage, a large-scale coarse mesh is forced at the open boundary by tidal constituents to propagate long waves and currents across the domain and towards the coastal regions. Meteorological forcing is applied during the final days of the spin-up period and throughout the simulation of interest. The coarse mesh simulation produces forecast results on the coastal ocean side of the estuary of interest and generates the time series boundary conditions for the stage two simulation. This coarse mesh does not feature any high-resolution coastal features. In the second stage, the fine mesh is forced with boundary conditions from the coarse mesh at open boundaries and meteorology over the duration for which hydrodynamic prediction is going to be made. The tool allows for a tide-only spin-up simulation on the fine mesh before applying the meteorology. The stage two simulation employs a fine-resolution mesh to resolve the more complex geometry and flow features inside a coastal estuarine system. Based on the geometry and geography of the domain, surface elevations of the fine mesh may need a short spin-up time. For storm surge and wave forecasting, as will be discussed in the case studies section, a 2D barotropic circulation model coupled to a phase-averaged wave model is applied in both coarse mesh simulation and fine mesh simulation. However, the physics of the coarse mesh and fine mesh do not need to match. Depending on the physical processes of study, any combination of model types can be applied such as 2D barotropic, 3D baroclinic, water quality model, and/or sediment transport.

### 3.2. Efficiency improvements

Continuous single-domain meshes take advantage of the grid flexibility of unstructured (FE in this study) methods. The mesh size function smoothly varies across the domain between regions of high-resolution and coarse-resolution. The necessity for gradually changing spatial resolution requires employing high-resolution in regions away from the fine-resolution areas. Nesting techniques further improve the efficiency of FE methods by allowing a large discontinuity in the mesh size function at interfaces of the coarse mesh and fine mesh. In other words, the coarse mesh is designed to deliberately remove high-resolution regions and to be as coarse as possibly configured while retaining accuracy along the open coastal region of study. This strategy allows for a coarser resolution along the coastal ocean boundary and in those areas of the mesh that smoothly connect the higher resolution coastal regions to the coarser resolution deep-ocean. Therefore, in coarse mesh simulation, the total number of nodes is expected to be greatly reduced over the conventional domain. The wall-clock time needed to spin up the tides and limited meteorology is significantly reduced.

Most FE-based models with a spatially varying grid resolution use a spatially constant time step, which is restricted by the smallest element size in the mesh. By implementing a nesting technique, we attempt to mitigate such inefficiency by splitting the geographical domain into two regions with different resolutions. While the fine mesh still requires the same minimum time step as the continuous single-domain approach, a significantly larger time step is allowed in the coarse mesh simulation.

Also, the nesting technique makes it possible for applying different physics in the coarse mesh and fine mesh. For example, in the case of a 3D circulation study inside an estuary, it may be unnecessary to perform 3D simulations outside the estuary. In this case, the nesting

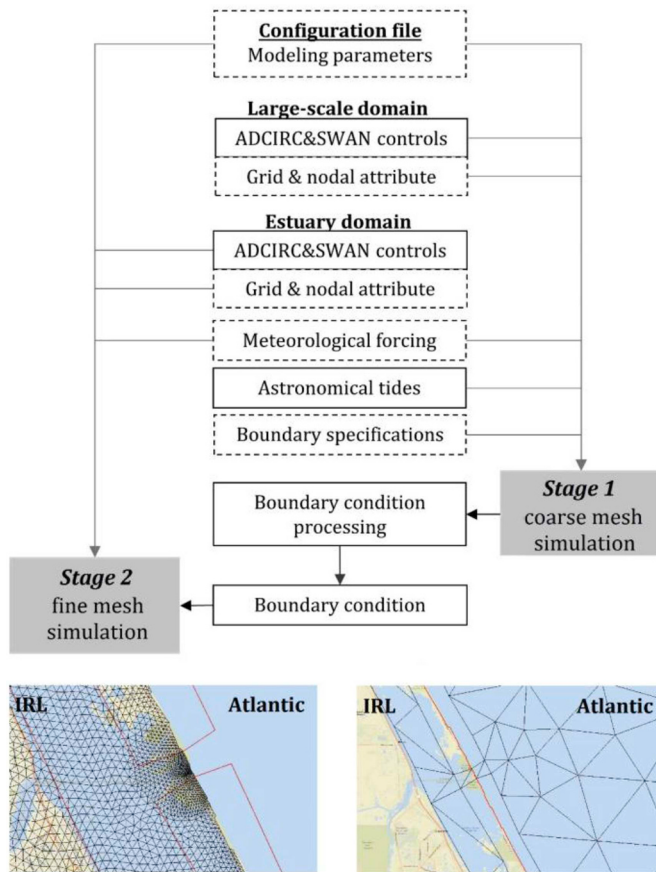


**Fig. 1.** Workflow of the *Multistage*. Solid boxes are either fixed components or generated in the process. Dashed boxes are input variables. Subsets of a coarse mesh (right) and a fine mesh (left) demonstrating the discontinuity of the mesh size function around Sebastian Inlet that connects the Indian River Lagoon (IRL) to Atlantic Ocean on the east coast of central Florida. Brown and red lines in each subset depict the active and inactive boundaries. In the fine mesh subset, for example, the red lines show the boundaries of the coarse mesh.

technique allows for a 2D barotropic run on the coarse mesh that produces boundary condition for a 3D baroclinic simulation of an estuary. In the case of coupling a circulation model to a wave model, the nesting technique makes it more feasible to couple the coarse mesh representing the deep ocean to a deep ocean wave model while the fine mesh representing a coastal estuary applies a shallow water wave model. *Multistage* also allows users to selectively enable wave models on the coarse or fine meshes.

### 3.3. Automation

Fig. 1 shows the workflow of the *Multistage* software, major components, and subsets of a coarse mesh and a fine mesh around Sebastian Inlet (the inlet connects the Indian River Lagoon (IRL) system to the Atlantic Ocean on the east coast of central Florida). The software consists of the main script for driving the system, configuration files, and modular programs scripted in Bash, Perl, and FORTRAN. For implementing the nesting technique as an automated tool, we took advantage of the ADCIRC Surge Guidance System (ASGS), a real-time storm surge and wave forecasting system created by Fleming et al. (2008). Real-time application of *Multistage* can be analogized to a branch of ASGS specifically designed for coastal estuarine system forecasting. For consistency within the ADCIRC community, similar approaches are applied in scripting the tool where modules and their interactions are either identical to those of ASGS (e.g., tide-generating modules) or adjusted for nesting applications (e.g., main script, control

file generator). There is also a new component added for generating the boundary condition file from the coarse mesh simulation, and a few auxiliary scripts for performing miscellaneous tasks. The *Multistage* tool consists of external and internal components. External components are variables and must be adjusted and customized by users for the study. Internal components are either fixed parts of the system or created by the system in the process. In brief, the system consists of the main driver script that initiates the simulation and proceeds by calling modular scripts to carry out specialized function(s).

### 4. Case studies

To evaluate the system for real-time applications, two estuarine systems, and associated test cases are selected: Charlotte Harbor/San Carlos Bay (SCB) forced by Hurricane Charley in 2004 in West Florida, and the Indian River Lagoon (IRL) forced by Hurricane Matthew in 2016 in East Florida. We will refer to these cases as SCB-Charley and IRL-Matthew. Meteorological events are selected based on the geographical path of their passages, and availability of storm information. The unique geographic location and extension of each estuarine system provide suitable testing scenarios. Port Charlotte Harbor/San Carlos Bay is located in West Florida between 26.35°N and 27.11°N. The system is connected to the Gulf of Mexico through Gasparilla, Boca Grande, Captiva, Redfish passes to the north, and San Carlos Bay entrance, Big Carlos and New passes to the south. The Indian River Lagoon is located between 26.89°N and 29.10°N along the east coast of Florida connecting to the Atlantic Ocean through 5 inlets: from north to south, Ponce, Sebastian, Fort Pierce, Saint Lucie, and Jupiter Inlets. Model forcing types include astronomical tides and mesoscale meteorology. Storm information is obtained from the National Hurricane Center (NHC) best track advisory and used to force a parametric dynamic Holland wind model coded as a subroutine in ADCIRC to generate winds and pressure fields (Fleming et al., 2008). The total length of simulations is set to 22 days in SCB-Charley (a 17-day tidal spin-up and a 5-day event simulation) and 11 days in IRL-Matthew (a tidal 7-day spin-up and a 4-day event simulation). The required tidal spin-up times were determined in previous work. For the fine mesh simulation, *Multistage* solutions were compared against single-domain solutions in order to establish the required model spin-up time. As presented in preliminary studies, a spin-up time of two days was found to be sufficient for case study one domain (SCB), and a spin-up time of one day for the case study two domain (IRL) (Taeb and Weaver, 2017). Spin-up simulations on the fine mesh are forced with meteorology and boundary conditions that contain storm-induced coastal impacts and tides.

#### 4.1. Assessment

We assess the performance of the applied nesting technique regarding model solution deviation from the single-domain technique and forecast runtime reduction. The deviation of the solution (DS) is calculated over the spatial region shared by the fine mesh of *Multistage* and the high-resolution coastal estuary of the single-domain, Eq. (1). The single-domain approach has been applied by the ADCIRC community with great success (Bacopoulos et al., 2012; Chen et al., 2007; Forbes et al., 2010; Olume et al., 2011; Sebastian et al., 2014; Westerink et al., 2008). In the absence of measured data against which the model can be compared, we assume that presenting a spatially and temporally averaged deviation from the single domain technique will give a sense of the reliability of the *Multistage* system. We calculate deviations as a supplementary measure to model-observation comparisons that will be presented later, regarding the sparse observation data.

The model output interval is set to 1800 s, providing time-dependent DS. The DS is averaged over output time snaps, Eq. (2), representing an average deviation over space and period of hydrodynamic simulations.

$$DS = \frac{\sum_{j=1}^{N_N} |Q_{Sj} - Q_{mj}|}{N_N} \quad (1)$$

$$DST = \frac{\sum_{t=1}^{N_TS} DS_t}{N_TS} \quad (2)$$

Where  $Q_S$  and  $Q_m$  represent the model solution of single-domain and *Multistage*, respectively. Index “j” indicates the number of the computational node of the fine mesh.  $N_N$  is the total number of computational nodes that are in common between two meshes and are active (wet).  $N_{TS}$  is the number of time snaps at which model solutions are output.

Forecast time reduction will be obtained by defining FTR following the relation in Eq. (3).

$$FTR = \frac{T_s - T_m}{T_s} \times 100 \quad (3)$$

Where  $T_s$  and  $T_m$  are total time of forecast using single-domain and *Multistage* approach, respectively. Total time does not include domain tidal spin-up simulations.

#### 4.2. Model setup

The same model parameters are specified for the *Multistage* and single-domain simulations throughout the study. We apply the barotropic 2-Dimensional Depth-Integrated (2DDI) ADCIRC construct using the lumped GWCE. Governing equations are described in spherical coordinates and transformed into Cartesian coordinates before discretization. A quadratic bottom friction law is applied that varies spatially and temporally based on the roughness (Manning's  $n$ ) value generated by an ADCIRC utility program. ADCIRC reads in Manning's  $n$  values from the nodal attribute file, with a prescribed  $n = 0.02$  in water. Over land, the parameter is determined from the National Land Cover Dataset (NLCD) (Arcement and Schneider, 1989; Luettich and Westerink, 2004; Fry et al., 2011). A weighting factor,  $\tau_0$ , between the primitive and wave contributions in the GWCE is determined at each computational node based on velocity, depth, and grid spacing. The Coriolis parameter is set to be spatially varying, computed from the y-coordinate of the computational nodes. From results obtained in our previous work (not shown here) (Taeb and Weaver, 2017) and the experience gained in the course of this study, a two-minute time-interval is applied as the boundary condition time step. Coupled ADCIRC + SWAN simulations have a coupling interval of 1200 s, the same as the SWAN time step size. In addition to water level, wind, and currents, SWAN is configured to read bottom friction computed by ADCIRC. SWAN is run in the third generation mode, with applied white-capping according to Komen et al. (1984). Depth-induced wave breaking in shallow water is activated in SWAN with default options and values. The iterative computation in SWAN is terminated if the absolute change in  $H_s$  from one iteration to the next is less than 0.005 m or the relative change in  $H_s$  from one iteration to the next is less than 0.01 m and the curvature of the iteration curve of  $H_s$  normalized with  $H_s$  is less than 0.005. More than 95% of all wet grid points need to fulfill these two conditions. SWAN is run in non-stationary mode, where a four-iteration computation is specified before moving to the next time step. The lower and upper limit of the frequency range used for computing integral parameters are set to 0.031 Hz and 1.42 Hz, respectively (Booij et al., 2004).

We conduct a series of studies on coarse mesh development in which the original mesh and two configurations of an onshore-extended coarse mesh are tested. Boundary conditions produced by modified versions of the coarse meshes are compared between an ADCIRC only, and a coupled ADCIRC + SWAN runs. Following the coarse mesh development section, for each case study, we performed four sets of validation simulations. Each set of simulations applies the same model parameters for the single-domain simulation and the nesting simulation. The first set of simulations, Table 1 row 1, use only the ADCIRC

**Table 1**

Four series of validation simulations performed for both case studies. A indicates an ADCIRC run, and A + S indicates a coupled ADCIRC + SWAN run. In the last row, “N”s indicate that corresponding simulations are discarded.

series	Single-domain		Nesting technique		
	spin-up	event	Coarse spin-up	Coarse event	Fine
			Model type	Model type	
1	A	A	A	A	A
2	A	A + S	A	A	A + S
3	A	A + S	A	A + S	A + S
4	A	A + S	N	N	A + S

model. The second set, Table 1 row 2, uses the coupled ADCIRC + SWAN, but the coarse mesh simulation is run with ADCIRC only. The third set of simulations, Table 1 row 3, uses ADCIRC + SWAN for the single-domain and both coarse mesh and fine mesh simulations. The fourth set of simulations, Table 1 row 4, highlights the importance of accounting for the storm-induced effects in the boundary condition. This simulation is performed by *Multistage* with coarse mesh simulation turned off, and the open boundaries are forced with tide only.

#### 4.3. Coarse mesh development

In coastal modeling, it is essential to account for the interaction between coastal estuaries and coastal oceans. This interaction is accounted for in continuous single-domain and in nesting applications where the fine mesh is extended far enough offshore. Offshore extension of a coastal estuary can add significant computational nodes to the fine mesh simulation. The IRL system, for example, is 250 km long along the coast. Offshore extension of the IRL fine mesh to areas where the bathymetry is well-represented by the coarse mesh would at least double the number of computational nodes. The increase in nodes and the small time step needed for the high resolution would result in no significant difference in runtime between a single-domain and a nesting technique. Alternatively, we propose to extend the coarse mesh into coastal estuaries and to resolve the region by a coarse representation.

We adopt the east-coast 1995 (ec95) (Mukai et al., 2002) mesh as the basis for developing the coarse meshes. The ec95 is modified at the locations bordering the open boundaries of the fine mesh of interest. Custom coarse meshes are developed for each target coastal estuary. These custom meshes contain increased resolution in the region neighboring the fine meshes. The depth of the nodes in the coarse mesh that correspond to the boundaries in the fine mesh is set to match the elevations of the fine mesh boundary.

Results from the initial simulations, in which resolution of the coarse mesh was not increased to include the coastal estuaries, indicated that the model was not capable of correctly capturing certain flow features near the open boundary. This deficiency is clearly demonstrated in the SCB-Charley case. Fig. 2(a) is a schematic time series of surface elevation during hurricane Charley's passage through Boca Grande Pass. As the storm eye approaches the Pass, the flow is offshore (because of combined suction of the low pressure of the eye and the wind direction) causing an initial set-down in water level. This set-down is, to some extent, compensated with an offshore flow out of the estuary, Fig. 2(b). The exclusion of the coastal estuary in the coarse mesh does not allow for this flow feature, Fig. 2(c), leading to an overestimated set-down as the storm approaches, and overestimated set-up when the storm eye is passing the inlet.

To mitigate such exaggerated variations, we modify the original coarse mesh, Fig. 3(a), to cover the estuary of study by a coarse representation, Fig. 3(b). Improvements in boundary condition accuracy are evaluated visually, and also quantitatively by Root-Mean-Square Deviation (RMSD), which is a measure of the difference between the

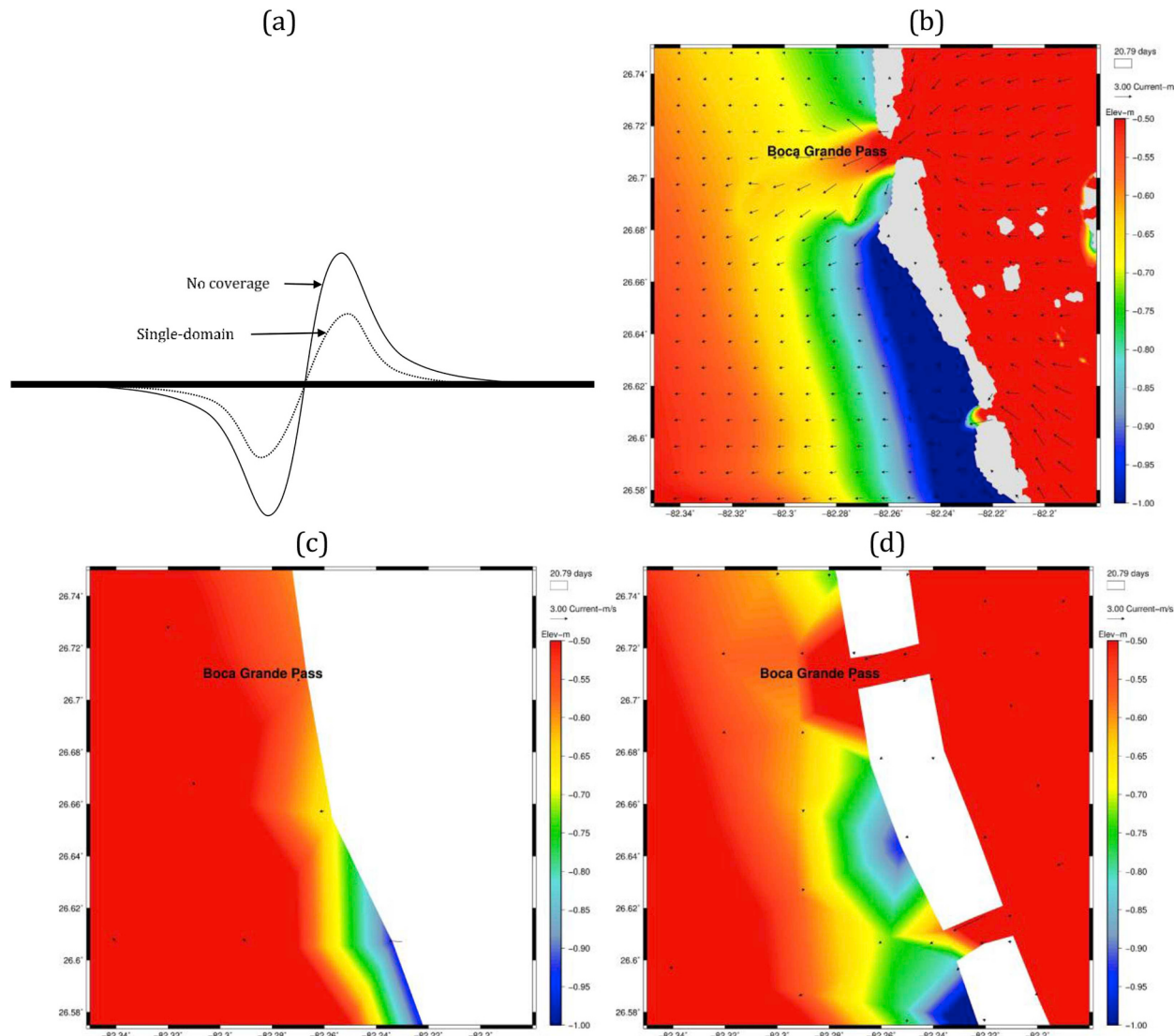


**Fig. 2.** (a) Symbolic surface elevation time series at Boca Grande Pass in case of accounting for (dotted line), and in case of ignoring the impact of the estuary outflow on the coastal water (solid line). The offshore flow (plume) of the estuary is illustrated in (b) using vectors from a single-domain simulation and is compared with (c) the coarse mesh with no estuary coverage, and (d) the resulted coarse mesh with coarsely resolved estuary. Subplots (b), (c), and (d) are corresponding to August 13, 2004, 19:00 UTC.

truth and boundary condition produced by the coarse mesh. Due to lack of observational data at the exact locations of the open boundaries, the surface elevation predicted by the single-domain run is assumed to be the true solution. Including the estuary is most effective when three computational nodes are used to represent the passes, Fig. 3(b) (25% improvement in RMSD) except at San Carlos Bay entrance where two nodes are employed. We compare the surface elevation boundary condition predicted by each coarse mesh against the single-domain solution at two open boundary locations, Boca Grande Pass, Fig. 3(c), and San Carlos Bay entrance, Fig. 3(d). Including the estuary in the coarse mesh is shown to damp the overestimated set-downs/set-ups which were illustrated in Fig. 2(a). The results indicate the importance of including the coarsely resolved coastal estuary in the coarse mesh. In the development of the modified coarse mesh, a minimum grid spacing of  $\sim 0.009^\circ$  was not exceeded to avoid reducing the time step. The resulting coarse mesh captures the bulk characteristics of the flow through Boca Grande Pass, Fig. 2(d), and improves the predicted increase in water level in the nearshore coast between longitudes  $82.28^\circ\text{W}$  and  $82.34^\circ\text{W}$ , Fig. 2(d). Evaluating the different configurations for the coarse mesh was conducted by ADCIRC, and the single-

domain run is performed by the coupled model. A final series of simulations are carried out on the coarse mesh with no estuary coverage and also coarsely resolved estuary by applying the coupled ADCIRC + SWAN model. This suite of simulations is intended to assess the applied model type for boundary condition accuracy. When the estuary is not represented in the coarse mesh, the time series of predicted boundary conditions are overestimated by the ADCIRC + SWAN run, Fig. 3(c and d). For the coarsely resolved estuary case, the ADCIRC + SWAN run shows no outperformance over the ADCIRC-only run, for hurricane Charley, but could be significant for other storms.

The resulting coarse mesh developed for the IRL does not cover the entire region. The IRL is a long narrow, shallow estuarine system extending 250 km along the Florida east central coast. Regarding circulation, the IRL can be divided into sub-regions, each acting as an enclosed basin rather than an integrated system (Schultz, 2008). Among numerous different configurations, the best results were achieved when the coastal estuary is approximated by five sub-regions, Fig. 4(a). For IRL-Matthew, minor improvements are obtained by representing the estuary in the coarse mesh. Only at Sebastian Inlet, a similar overestimating of predicted water level shown in Fig. 2(a) is seen after the

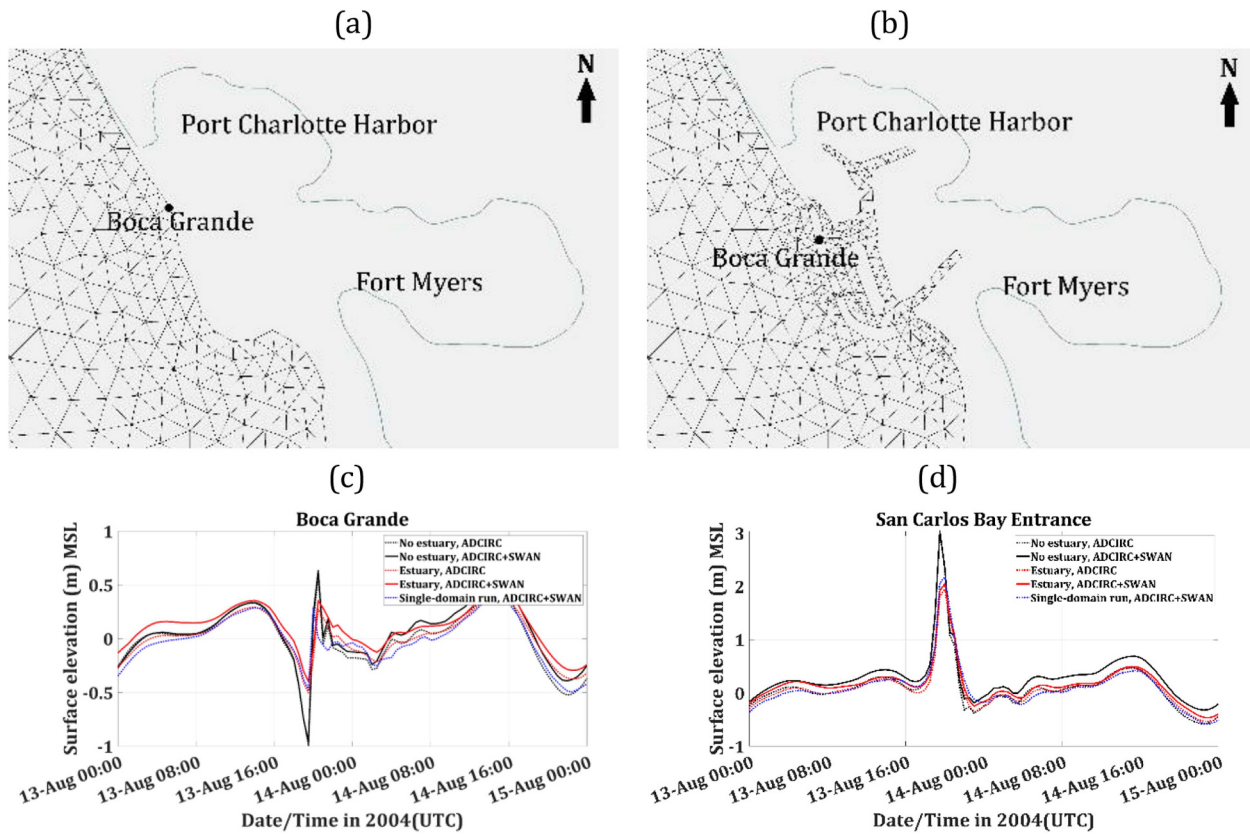


**Fig. 3.** (a) Original coarse mesh, ec95, (b) Resulting coarse mesh extended into the IRL. Time series water level predicted by the single-domain run (blue dotted lines), the coarse mesh with no coverage for the estuary (dotted black lines for ADCIRC-only runs and solid black lines for the coupled runs), and the coarse mesh with the estuary inclusion (dotted red lines for ADCIRC-only run and solid red lines for the coupled runs) are presented at (c) Boca Grande Pass, and (d) San Carlos Bay Entrance.

storm has passed the inlet. By including the IRL in the coarse mesh, offshore estuary flow is allowed at the inlet improving the accuracy of the predicted water level, Fig. 4(b).

On the other hand, at Saint Lucie inlet, for example, there is no significant difference between model runs whether or not the coastal estuary is resolved in the coarse mesh, Fig. 4(c). In contrast to SCB-Charley, improvements, although small, are achieved at open boundaries by applying coupled ADCIRC + SWAN model in the coarse mesh simulation. At Fort Pierce Inlets, for example, the coupled ADCIRC + SWAN run on the coarse mesh with the inclusion of the estuary helped improve the boundary condition at the peak of the storm surge, Fig. 4(d).

The coarse mesh is an essential component of the *Multistage* regarding both accuracy and efficiency. Model instabilities occasionally are observed in some regions in the Caribbean Sea where geometry and bathymetry have sharp gradients as well as northwest and southwest of the Gulf of Mexico. With insufficient grid points, or/and improper mesh configuration, these regions are prone to spawn instabilities that lead to simulation termination, or impaired hydrodynamic predictions for the coastal ocean. While making relative improvements, coarse mesh development is still an ongoing process in our work. The present method for including the estuaries is not yet reliable enough and that a further refinement or smoother transition in mesh size is deemed necessary to obtain more reliable results in coastal areas.

Moreover, coarse but proper representation of the estuary of study in the coarse mesh can significantly improve the boundary condition accuracy. In general, a well-designed coarse-resolution mesh is a key component in the application of the *Multistage* system.

## 5. Results

The performance of the *Multistage* system tested on two case studies is presented in this section and comparisons are made within models and between models and observations. Time series of surface elevations produced are compared against observation in Fig. 5, at National Oceanic and Atmospheric Administration (NOAA), Florida Department of Environmental Protection (FDEP), Collaborative Science, Technology, and Applied Research (CSTAR), and the United States Geological Survey (USGS) stations.

The results obtained from the nesting technique are in agreement with the single-domain run and the observed data at Fort Myers, Fig. 5(a), and Matanzas Pass, Fig. 5(b). Even though the Fort Myers station is located nearly 30 km from the nearest open boundary, San Carlos Bay entrance, peak water levels during the storm passage is underestimated when the coarse mesh simulation is turned off. Matanzas Pass is located inside the estuary between Big Carlos Pass and San Carlos Bay entrance. The inaccuracy in water level prediction is more significant at Matanzas Pass than other stations when the coarse mesh simulation is turned off. Boca Grande station, Fig. 5(c), is located on the northern edge of the Boca Grande Pass a few hundred meters from the inlet inside the lagoon. The solution produced by *Multistage* shows discrepancies at this station. Even the single-domain run is not able to predict the initial storm-induced water level setup. However, the subsequent set-down is reproduced accurately, Fig. 5(c).

For IRL-Matthew, model to observation comparisons are made at two stations that are well-represented by the mesh. Results indicate that water levels predicted by both single-domain and nesting techniques match up well to the observations at those locations. Both techniques underestimate the peak water level at the southern station, Sebastian

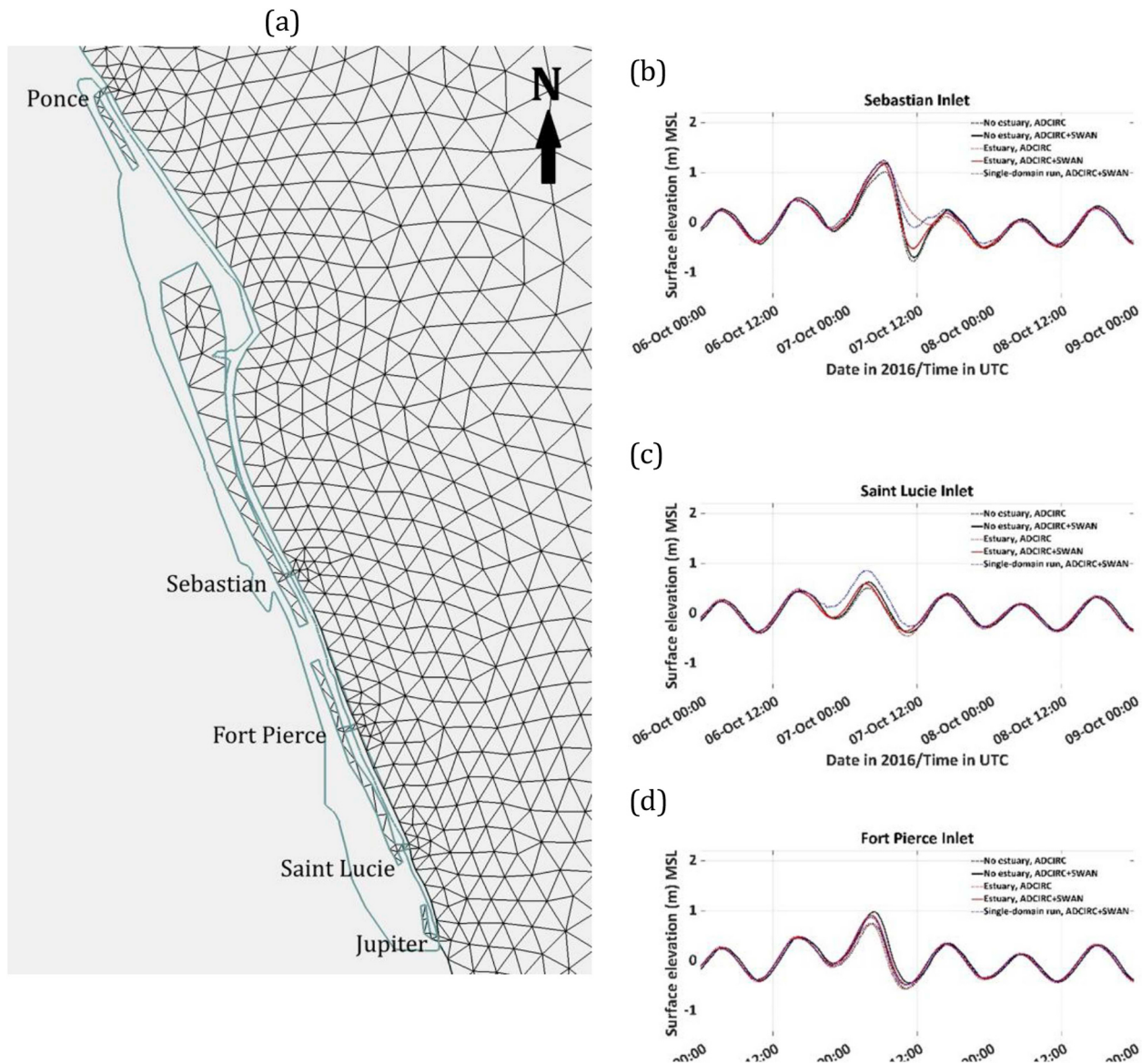


**Fig. 4.** (a) Resulting coarse mesh extended into the IRL. Time series water level predicted by the single-domain run (blue dotted lines), the coarse mesh with no coverage for the estuary (dotted black lines for ADCIRC-only runs and solid black lines for the coupled runs), and the coarse mesh with the estuary inclusion (dotted red lines for ADCIRC-only run and solid red lines for the coupled runs) are presented at (b) Sebastian, (c) Saint Lucie and (d) Fort Pierce Inlets.

fishery pier which is just west of the Sebastian Inlet, Fig. 5(d). The underestimate could result from the use of a parameterized wind and pressure field as well as the absence in the model of storm-induced rainfalls that increased the discharge of Saint Sebastian River near the Sebastian station (from 2  $m^3/s$  to 20  $m^3/s$  recorded by USGS station 02251500). For the test run in which the open boundaries were forced by tide only (no information from the coarse mesh run applied at the open boundaries of the nested domain), the water level peak is significantly underestimated at Sebastian fishing pier, Fig. 5(d). It is noteworthy that there is no significant difference in predicted water levels between these simulations at Lansing Island, Fig. 5(e). The distance between this station and the nearest open boundary, Sebastian Inlet, is 40 km, nearly the same distance between Fort Myers and the nearest open boundary in the case study one. However, from SCB-Charley, we found that the water level peak in areas far from open boundaries are not captured if the wind-induced water level variations are not applied at the open boundaries. This can be explained in part by the geometry and orientation of the IRL system. The IRL system is comprised by four sub-lagoons that are connected to each other through narrow canals or

conveyances. The system circulation pattern is interrupted at the interfaces of two adjoining sub-lagoons. The Lansing Island station is located in the south of Banana River, one of the four sub-lagoons of the IRL system that is connected to the Indian River by two narrow channels. These connections are narrow and can disrupt the circulation between two sub-lagoons. The IRL circulation pattern is also interrupted by 13 causeway/bridges that divide the IRL system into sub-basin compartments (Schultz, 2008). Two of these causeways (Melbourne Causeway and Eau Gallie Causeway) are located between the Lansing Island station and Sebastian Inlet. Moreover, the IRL system is shallow and narrow oriented parallel to the coastline while the Port Charlotte Harbor/San Carlos Bay system is oriented inshore.

We found no historical data of wave heights recorded inside the coastal estuaries for comparing model-predicted significant wave heights ( $H_s$ ) with observational data. Thus, the comparison of  $H_s$  is made between model predictions by the single-domain and the nesting technique, illustrated on the right axes of Fig. 5 plots. The comparison for wave height indicates 2–7 cm underestimate at the peak by the nesting technique at Fort Myers, Fig. 5(a) and a 5 cm underestimate at

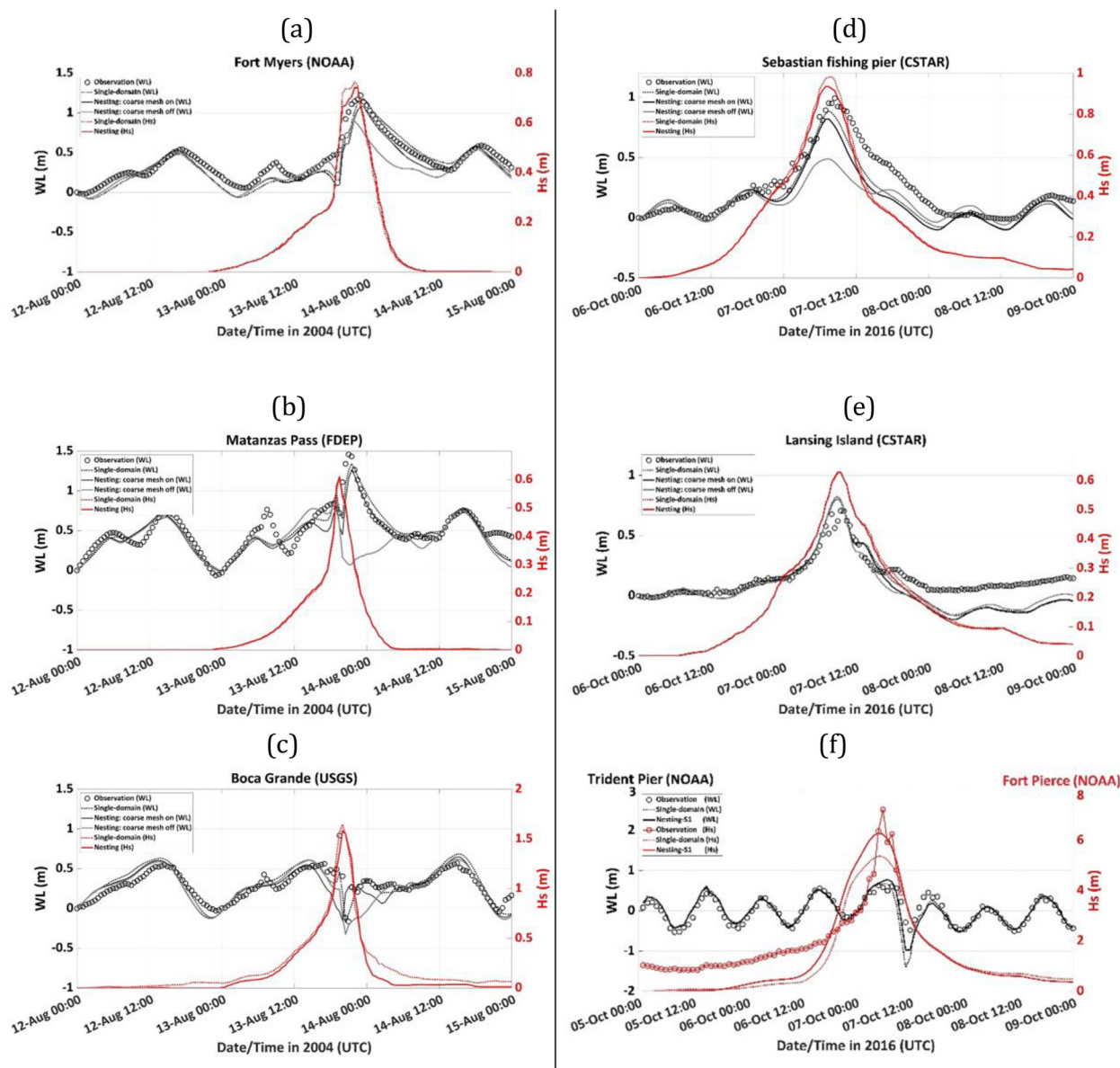


**Fig. 5.** Comparison of time series of water level (WL) predicted by the nesting technique when the coarse mesh simulation turned on i.e. the coarse mesh is run first to provide boundary conditions (black solid lines), when the coarse mesh turned off i.e. no boundary forcing is applied to open boundaries of the fine mesh (gray lines), the single-domain runs (black dotted lines), and observations (black circles), predicted  $H_s$  by the single-domain runs (solid red lines), and by the nesting runs (dotted red lines) for SCB-Charley at (a) Fort Myers (NOAA) ( $26.6482^\circ N, 81.8722^\circ W$ ), (b) Matanzas Pass ( $26.4349^\circ N, -81.9113^\circ W$ ), and (c) Boca Grande (USGS) ( $26.7231^\circ N, 82.25762^\circ W$ ), and for IRL-Matthew at (d) Sebastian fishing pier ( $27.8088^\circ N, 80.4617^\circ W$ ), (e) Lansing Island ( $28.159227^\circ N, 80.609215^\circ W$ ), (f) Trident Pier (NOAA) for water level only ( $28.4117^\circ N, 80.594^\circ W$ ) and Fort Pierce (NOAA) for  $H_s$  only ( $27.5550^\circ N, 80.217^\circ W$ ), with red circle for observational  $H_s$ .

**Table 2**

Model solution deviation of nesting technique from single domain solution (average over computational space) represented as an average over output time snaps (Ave), standard deviation (std), and the maximum deviation (max) in terms of surface elevation, currents, and significant wave height ( $H_s$ ).

Case	Surface Elev. deviation (cm)		Current deviation (cm/s)		$H_s$ deviation (cm)	
	Ave ± std	Max	Ave ± std	Max	Ave ± std	Max
SCB-Charley	$4.9 \pm 2.5$	10.8	$2.3 \pm 1.2$	8.5	$0.8 \pm 0.9$	5.2
IRL-Matthew	$4.0 \pm 2.7$	10.1	$3.6 \pm 1.8$	8.4	$1.7 \pm 0.9$	3.7

the peak at Sebastian Fishing Pier, Fig. 5 (d). The underestimate at Sebastian Pier could be resolved if the Sebastian Inlet open boundary was forced by wave information. At other stations inside the coastal

estuaries, the  $H_s$  predictions by the fine mesh agree strongly well with time series of  $H_s$  computed by the single-domain runs, Fig. 5 (b, c, and e).

Coarse mesh validations are limited only to IRL-Matthew in this study due to lack of observational stations or failure of stations located in the domains during the events of study. The coarse mesh simulation was validated for the predicted water level at Trident Pier (NOAA) tidal station on the east coast of Florida, Fig. 5(f) left axis, and for the predicted  $H_s$  at NOAA buoy station 41114 – offshore from Fort Pierce (FL), Fig. 5(f) right axis. Trident Pier is located inside the Port Canaveral on the ocean side of the IRL system and Fort Pierce buoy is located 11.3 km northeast of Fort Pierce Inlet at a depth of 16 m. The coarse mesh simulation outperforms the single-domain run in predicting the maximum set-down of water level at Trident Pier. Both techniques underestimate the maximum wave height at Fort Pierce and predict an early increase in  $H_s$ . The model deviation from the observations before and

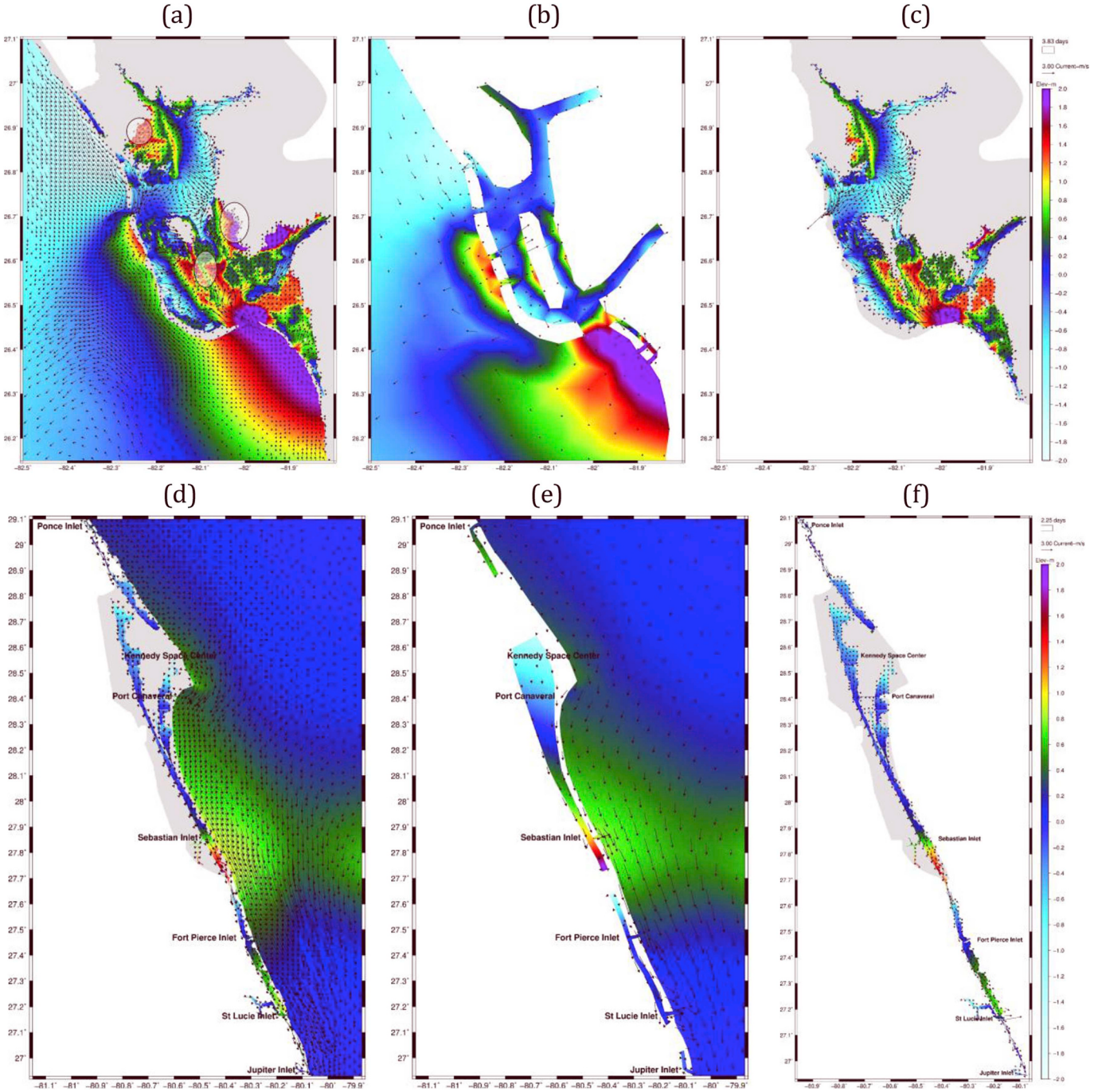


**Fig. 6.** Comparison of 2D contours of predicted water levels overlaid with current velocity vectors between the single-domain and the nesting techniques. (a) and (d) are single-domain simulations, (b) and (e) are coarse mesh simulations of the nesting technique, and (c) and (f) are fine mesh simulations of the nesting technique for San Carlos Bay corresponding to August 13, 2004, 20:00 UTC and the IRL system corresponding to October 7, 2016, 06:00 UTC, respectively. Highlighted white hatched circles in Fig. 6(a) depict three regions inside the estuary that are predicted to be flooded by the single-domain simulation, but not by the fine mesh simulation of nesting technique.

after the storm passage is due to the parametric Holland-type forcing used to simulate the storm that does not fill out the wind field before the hurricane arrives and after the hurricane passes. Model performance during the storm will also suffer from the parameterized forcing. Note that the observational  $H_s$  is available until October 7, 2016, 12:00 UTC. Coarse mesh simulation validations are insufficient to identify any physical processes that might be predicted differently between the single-domain and the nesting technique. More validation efforts need to be carried out for the performance of the coarse mesh simulations.

Table 2 presents the model solution deviations of the nesting

technique from the single-domain run, Eqs. (1) and (2). On average, the predicted surface elevation deviates less than 5 cm from the single-domain solution over the interior region of the domain, with a maximum value of 10.8 cm for SCB-Charley. The average deviation of current velocity is 2.3 cm/s and predicted significant wave height deviates by 0.8 on average. Results show a smaller deviation in the predicted water level in IRL-Matthew (an average of 4 cm and a maximum of 10.1 cm) than seen in SCB-Charley, while current velocity and significant wave heights have a larger average deviation of 3.6 cm/s and 1.7 cm, respectively, Table 2. The calculated deviation does not

**Table 3**

Comparison of the simulations performed by the single-domain method and the nesting technique. Columns titled with type indicate if ADCIRC (A) is run, or coupled ADCIRC + SWAN (A + S) is applied. The last column is the FTR calculated by Eq. (3). Spin-up simulations runtimes (of both methods) are not taken in runtimes columns and FTRs calculations. Computations are performed on a desktop research computer in parallel using 45 processors.

#CPU	Single-domain			Nesting			FTR %
	spin-up	event		Coarse spin-up	Coarse event	fine	
	17days	5days		17days	5days	5days	
Type	Runtimes	Type		Type		Runtimes	
SCB-Charley	45	A	A	3h	A	A	1h 65.5%
	45	A	A + S	11h 28m	A	A	4h 40m 59.3%
	45	A	A + S	11h 28m	A	A + S	4h 40m 53.9%
#CPU	spin-up	event		S1 spin-up	S1 event	S2	FTR%
IRL-Matthew	7days	4days		7days	4days	4days	
	Type	Runtimes	Type	Type			Runtimes
	45	A	A	1h 33m	A	A	17m 81.7%
IRL-Matthew	45	A	A + S	5h 14m	A	A	1h 80.8%
	45	A	A + S	5h 14m	A	A + S	1hr 29m 71.6%

necessarily represent the inaccuracy of solutions produced by *Multistage*. However, by comparing single-domain and nesting solutions with available gaging stations, single-domain runs performs slightly better than the nesting method, particularly at regions close to open boundaries, Fig. 5 (c and d).

We closely examined 2D contour plots of the predicted water level, current velocities and wave heights to identify any distinct physical processes that might be treated differently by the nesting technique compared to the single-domain simulation. For SCB-Charley, we illustrate a snapshot of predicted surface elevation overlaid with depth-integrated current velocity vectors on August 13, 2004, at 20:00 UTC, Fig. 6(a, b, and c). As shown in Fig. 6 (a), the single-domain simulation predicts a strong inflow at San Carlos Bay and strong outflow in Boca Grande. The magnitude of the current velocity vectors indicates that these flows are not well-captured by the coarse mesh at the interfaces, Fig. 6(b) while fine mesh simulation does capture these flows, Fig. 6 (c). At this time, the storm surge had arrived at San Carlos Bay, but the narrow entrance does not allow for added water mass (surge) to enter the estuary. Demonstrated in Fig. 6(a) from the single-domain run, the surge starts spreading at the entrance, part of that diverted inside the Bay through the bay entrance while the remaining is flowing in the north and south directions along the coast. The magnitude and geographical extent of the spread of surge are well-represented by the coarse mesh run; however, a slightly higher level of refinement is deemed to be essential for a better representation of the water levels in nearshore coastal waters.

At this time in the simulation, a significant difference in the geographical extent of predicted inundated regions starts evolving inside the estuary between the single-domain and fine mesh simulations. Highlighted white hatched circles in Fig. 6(a) depict three regions inside the estuary that are predicted to be flooded by the single-domain simulation, but not by the fine mesh simulation of nesting technique. The larger deviation of water level in SCB-Charley than IRL-Matthew, shown in Table 2, could be due to the different predictions for the extent of inundated regions between the single-domain run and the fine mesh simulation.

For IRL-Matthew, the snapshots are corresponding to October 7, 2016, 06:00 UTC, Fig. 6(d, e, and f) when the storm surge arrived at the Florida east central coast. The nesting technique captures general flow features for IRL-Matthew. The coarse mesh captures the magnitude and extent of the storm surge and the southerly current along the coast, Fig. 6(e). Comparing the 2D contours of the single-domain to the fine mesh water level, Fig. 6(d and f), the fine mesh simulation shows capability in capturing the water level set-down in North Indian River

(28.75° N latitude), the set-up in regions south of Sebastian inlet, and water level variations around causeways, Fig. 6(d and f). At Saint Lucie inlet, the underestimated boundary condition shown in Fig. 4(b) appears in the 2D contour of predicted water level, Fig. 6(f).

A summary of simulation lengths, spin-up, event, and total runtime are presented in Table 3 for each case study and technique. The first series of simulations is an ADCIRC only type. The largest forecast time reduction is associated with this type for both case studies, 65.5% for SCB-Charley and 81.7% for IRL-Matthew. To provide a wave forecast inside a coastal estuary, the ADCIRC + SWAN model is used in the event simulations of the single-domain, and the fine mesh simulations of *Multistage*. Compared to running ADCIRC only, FTR values are reduced to 59.3% and 80.8%. To provide a wave forecast on the ocean side of the coastal estuary, ADCIRC + SWAN is applied in the coarse mesh runs as well. Using the coupled model increases the total runtime, but the system still retains the tool scalability for ensemble modeling. Calculations reflect 53.9% and 71.6% forecast time reduction for this test case. Performing ensemble simulations will become practical and operational, benefiting from the computational efficiencies obtained by applying the *Multistage* system. Within the same CPU-hours required by a single-domain technique for performing one simulation, *Multistage* can perform two to three ensemble runs for SCB-Charley, and three to five for IRL-Matthew depending on the model type. Synthesized results are expected to improve the accuracy of prediction.

## 5. Conclusion

Conventional one-way nesting is applied within the framework of an unstructured ADCIRC model to improve the computational efficiency. The modeling processes are scripted into an automated software to facilitate the applications for offline simulations and future real-time ensemble forecasting, named *Multistage*. The results obtained from *Multistage* validation show significant improvements, with simulation runtime reductions of 54% to more than 80%. At the same time, the solution resulted in relatively small deviations compared to the conventional single-domain technique. Using the same CPU-hours required by the conventional single-domain technique, the *Multistage* system can produce 2-to-5 ensemble runs for the large-scale coarse mesh and the small-scale fine mesh. Alternatively, the savings in the computational cost can be used for running multiple fine meshes after a single coarse mesh run. This practice has applications in real time where a single coarse mesh is run first, and only the fine meshes that are in the path of a storm are activated.

One of the key factors in the *Multistage* system is the extension of the

coarse mesh onshore to include a representation of the coastal estuaries. The inclusion of a coarse representation of the estuary in the coarse mesh is critical in order to provide representative boundary conditions. Placing the open boundaries of the fine mesh near the coastline/ocean boundary of the inlets allows for a large discontinuity in the mesh size function at interfaces of the coarse mesh and the fine mesh. Results indicate that small-to-moderate improvements in the boundary condition accuracy can be achieved if the coarse mesh simulations are performed by the coupled circulation and wave model. In applications for which hydrodynamics inside an estuary are studied, an ADCIRC-only run for the coarse mesh could save significant computational cost and modeling efforts.

The assessment and development of *Multistage* are ongoing and focused on the real-time version of the system, boundary conditions/types, and improvements for the coarse mesh. Boundary nodes of the fine meshes can be forced with the non-periodic normal flow in ADCIRC which will be included in future versions. Wave information will also be added to the boundary condition forcing of the fine mesh. The present results illustrate that refinement of the coarse mesh resolution in nearshore areas, as well as the inclusion of tidal inlets, is important, but that the level of refinement is still subject for further research as the present methodology did not yet give reliable results for some inlets. We are working on establishing a robust algorithm for configuring the coarse mesh in the coastal regions of interest to ensure reliability at any open boundaries of a coastal estuary.

## Acknowledgments

We thank Dr. Steven Lazarus for his helpful feedback and his pearls of wisdom with us during this work, and for comments that greatly improved the manuscript. Work for this research was supported by NOAA Collaborative Science, Technology, and Applied Research (CSTAR) Program, grant #NA14NWS4680014.

## Appendix A. Supplementary data

Supplementary data to this article can be found online at <https://doi.org/10.1016/j.ecss.2018.09.020>.

## References

- Altuntas, A., Baugh, J., 2017. Adaptive subdomain modeling: a multi-analysis technique for ocean circulation models. *Ocean Model.* 115, 86–104. <https://doi.org/10.1016/J.OCEMOD.2017.05.009>.
- Arcement, G.J., Schneider, V.R., 1989. Guide for Selecting Manning's Roughness Coefficients for Natural Channels and Flood Plains.
- Bacopoulos, P., Dally, W.R., Hagen, S.C., Cox, A.T., 2012. Observations and simulation of winds, surge, and currents on Florida's east coast during hurricane Jeanne (2004). *Coast. Eng.* 60, 84–94. <https://doi.org/10.1016/J.COASTALENG.2011.08.010>.
- Baugh, J., Altuntas, A., Dyer, T., Simon, J., 2015. An exact reanalysis technique for storm surge and tides in a geographic region of interest. *Coast. Eng.* 97, 60–77. <https://doi.org/10.1016/J.COASTALENG.2014.12.003>.
- Blain, C.A., Cambazoglu, M.K., Kourafalou, V.H., 2009. Modeling the Dardanelles strait outflow plume using a coupled model system. *Ocean* 1–8. 2009, MTS/IEEE Biloxi-Marine Technol. Our Future. Glob. Local Challenges. IEEE. <https://doi.org/10.23919/OCEANS.2009.5422421>.
- Booij, N., Haagsma, I.J., Holthuijsen, L.H., Kieftenburg, A.T., Ris, R.C., Van Der Westhuysen, A.J., Zijlema, M., 2004. SWAN Cycle III Version 40.41 User Manual.
- Booij, N., Ris, R.C., Holthuijsen, L.H., 1999. A third-generation wave model for coastal regions: 1. Model description and validation. *Geophys. Res. Ocean.* 104, 7649–7666. <https://doi.org/10.1029/98JC02622>.
- Bunya, S., Dietrich, J.C., Westerink, J.J., Ebersole, B.A., Smith, J.M., Atkinson, J.H., Jensen, R., Resio, D.T., Luettich, R.A., Dawson, C., Cardone, V.J., Cox, A.T., Powell, M.D., Westerink, H.J., Roberts, H.J., 2010. A high-resolution coupled riverine flow, tide, wind, wind wave, and storm surge model for southern Louisiana and Mississippi. Part I: model development and validation. *Mon. Weather Rev.* 138, 345–377. <https://doi.org/10.1175/2009MWR2906.1>.
- Chassignet, E.P., Hurlburt, H.E., Smedstad, O.M., Halliwell, G.R., Hogan, P.J., Wallcraft, A.J., Baraille, R., Bleck, R., 2007. The HYCOM (HYbrid Coordinate Ocean Model) data assimilative system. *J. Mar. Syst.* 65, 60–83. <https://doi.org/10.1016/J.JMARSYS.2005.09.016>.
- Chen, C., Liu, H., Beardsley, R.C., 2003. An unstructured, finite volume, three-dimensional, primitive equation ocean model: application to coastal ocean and estuaries. *J. Atmos. Ocean. Technol.* 20, 159–186. <https://doi.org/10.1175/1520-0426.2003.020.0008.0001>.
- Chen, Q., Wang, L., Zhao, H., Douglass, S.L., 2007. Prediction of storm surges and wind waves on coastal highways in hurricane-prone areas. *J. Coast Res.* 1304–1317. <https://doi.org/10.2112/05-0465.1>.
- Dietrich, J.C., Dawson, C.N., Proft, J.M., Howard, M.T., Wells, G., Fleming, J.G., Jr., R.A.L., Westerink, J.J., Cobell, Z., Vitse, M., Lander, H., Blanton, B.O., Szpilka, C.M., Atkinson, J.H., 2013. Real-time forecasting and visualization of HurricaneWaves and storm surge using SWAN + ADCIRC and FigureGen. *Comput. challenges Geosci* 156, 49–70. Springer, New York, NY. <https://doi.org/10.1007/978-1-4614-7434-0>.
- Dietrich, J.C., Tanaka, S., Westerink, J.J., Dawson, C.N., Luettich, R.A., Zijlema, M., Holthuijsen, L.H., Smith, J.M., Westerink, L.G., Westerink, H.J., 2012. Performance of the unstructured-mesh, SWAN + ADCIRC model in computing hurricane waves and surge. *J. Sci. Comput.* 52, 468–497. <https://doi.org/10.1007/s10915-011-9555-6>.
- Dietrich, J.C., Zijlema, M., Westerink, J.J., Holthuijsen, L.H., Dawson, C., Luettich, R.A., Jensen, R.E., Smith, J.M., Stelling, G.S., Stone, G.W., 2011. Modeling hurricane waves and storm surge using integrally-coupled, scalable computations. *Coast. Eng.* 58, 45–65. <https://doi.org/10.1016/j.coastaleng.2010.08.001>.
- Fleming, J.J., Fulcher, C.W., Luettich, R.A., Estrade, B.D., 2008. A real time storm surge forecasting system using ADCIRC. *Estuar. Coast. Model.* 893–912.
- Forbes, C., Luettich, R.A., Mattocks, C.A., Westerink, J.J., 2010. A retrospective evaluation of the storm surge produced by hurricane Gustav (2008): forecast and hindcast results. *Weather Forecast.* 25, 1577–1602. <https://doi.org/10.1175/2010WAF2222416.1>.
- Fry, J., Xian, G.Z., Jin, S., Dewitz, J., Homer, C.G., Yang, L., Barnes, C.A., Herold, N.D., Wickham, J.D., 2011. Completion of the 2006 national land cover database for the conterminous United States. *Photogramm. Eng. Rem. Sens.* 77, 858–864.
- Funakoshi, Y., Hagen, S.C., Bacopoulos, P., 2008. Coupling of hydrodynamic and wave models: case study for hurricane Floyd (1999) hindcast. *J. Waterw. Port, Coast. Ocean Eng.* 134, 321–335. [https://doi.org/10.1061/\(ASCE\)0733-950X\(2008\)134:6\(321\)](https://doi.org/10.1061/(ASCE)0733-950X(2008)134:6(321)).
- Hallowell, G.R., Bleck, R., Chassaignet, E.P., Smith, L.T., 2000. Mixed layer model validation in Atlantic Ocean simulations using the Hybrid Coordinate Ocean Model (HYCOM). *Eos (Washington, DC)* 80, OS304.
- Harris, L.M., Durran, D.R., 2010. An idealized comparison of one-way and two-way grid nesting. *Mon. Weather Rev.* 138, 2174–2187. <https://doi.org/10.1175/2010MWR3080.1>.
- Hinkelmann, R., 2006. Efficient Numerical Methods and Information-processing Techniques for Modeling Hydro-and Environmental Systems. Springer Science & Business Media.
- Hope, M.E., Westerink, J.J., Kennedy, A.B., Kerr, P.C., Dietrich, J.C., Dawson, C., Bender, C.J., Smith, J.M., Jensen, R.E., Zijlema, M., Holthuijsen, L.H., Luettich, R.A., Powell, M.D., Cardone, V.J., Cox, A.T., Pourtaheri, H., Roberts, H.J., Atkinson, J.H., Tanaka, S., Westerink, H.J., Westerink, L.G., 2013. Hindcast and validation of Hurricane Ike (2008) waves, runup, and storm surge. *J. Geophys. Res. Ocean.* 118, 4424–4460. <https://doi.org/10.1002/jgrc.20314>.
- Ji, M., Aikman, F., Lozano, C., 2010. Toward improved operational surge and inundation forecasts and coastal warnings. *Nat. Hazards* 53, 195–203. <https://doi.org/10.1007/s10606-009-9414-z>.
- Komen, G.J., Hasselmann, K., Hasselmann, K., 1984. On the existence of a fully developed wind-sea spectrum. *J. Phys. Oceanogr.* 14, 1271–1285. [https://doi.org/10.1175/1520-0485\(1984\)014<1271:OTECAF>2.0.CO;2](https://doi.org/10.1175/1520-0485(1984)014<1271:OTECAF>2.0.CO;2).
- Luettich, J.R.A., Westerink, J.J., Scheffner, N.W., 1992. ADCIRC: an Advanced Three-dimensional Circulation Model for Shelves, Coasts, and Estuaries; Report 1, Theory and Methodology of ADCIRC-2DDI and ADCIRC-3DL (TR DRP-92-6).
- Luettich, R.A., Westerink, J.J., 2015. ADCIRC: a Parallel Advanced Circulation Model for Oceanic, Coastal and Estuarine Waters; User's Manual for Version 51.
- Luettich, R.A., Westerink, J.J., 2006. ADCIRC: a Parallel Advanced Circulation Model for Oceanic, Coastal and Estuarine Waters; User's Manual for Version 45.08.
- Luettich, R.A., Westerink, J.J., 2004. Formulation and Numerical Implementation of the 2D/3D ADCIRC Finite Element Model Version 44.XX. R. A., Luettich.
- Lyard, F., Lefevre, F., Letellier, T., Francis, O., 2006. Modelling the global ocean tides: modern insights from FES2004. *Ocean Dynam.* 56, 394–415. <https://doi.org/10.1007/s10236-006-0086-x>.
- Lynch, D.R., Gray, W.G., 1979. A wave equation model for finite element tidal computations. *Comput. Fluids* 7, 207–228.
- Mukai, A.Y., Westerink, J.J., Luettich Jr., R.A., Mark, D., 2002. Eastcoast 2001: a Tidal Constituent Database for the Western North Atlantic, Gulf of Mexico and Caribbean Sea. Coastal and Hydraulics Laboratory Tech. Rep. ERDC, US Army Corps of Engineers ERDC/CHL TR-02-24.
- Oey, L.-Y., Chen, P., 1992. A nested-grid ocean model: with application to the simulation of meanders and eddies in the Norwegian Coastal Current. *J. Geophys. Res. Ocean.* 97, 20063–20086. <https://doi.org/10.1029/92JC01991>.
- Olume, V., Ietric, J.C.D., Esterink, J.J.W., Ennedy, A.B.K., Mith, J.M.S., Ensen, R.E.J., Ijlema, M.Z., Olthuijsen, L.H.H., Awson, C.D., Uettich, R.A.L.J.R., Owell, M.D.P., Ardone, V.J.C., Ox, A.T.C., Tone, G.W.S., Ourtaheri, H.P., Ope, M.E.H., Al, D.E.T., 2011. Hurricane Gustav (2008) waves and storm Surge: hindcast, synoptic analysis, and validation in southern Louisiana. *Mon. Weather Rev.* 139, 2488–2522. <https://doi.org/10.1175/2011MWR3611.1>.
- Qi, J., Chen, C., Beardsley, R.C., 2018. FVCOM one-way and two-way nesting using ESMF: development and validation. *Ocean Model.* 124, 94–110. <https://doi.org/10.1016/J.JOC.2018.02.007>.
- Roland, A., Zhang, Y.J., Wang, H.V., Meng, Y., Teng, Y.C., Maderich, V., Brovchenko, I., Dutour-Sikiric, M., Zanke, U., 2012. A fully coupled 3D wave-current interaction model on unstructured grids. *J. Geophys. Res. Ocean.* 117, 1–18. <https://doi.org/10.1029/2012JC007952>.
- Schultz, S.T., 2008. Seagrass monitoring by underwater videography: disturbance

- regimes, sampling design, and statistical power. *Aquat. Bot.* 88, 228–238. <https://doi.org/10.1016/J.AQUABOT.2007.10.009>.
- Sebastian, A., Proft, J., Dietrich, J.C., Du, W., Bedient, P.B., Dawson, C.N., 2014. Characterizing hurricane storm surge behavior in Galveston Bay using the SWAN + ADCIRC model. *Coast. Eng.* 88, 171–181. <https://doi.org/10.1016/J.COASTALENG.2014.03.002>.
- Sheng, J., Greatbatch, R.J., Zhai, X., Tang, L., 2005. A new two-way nesting technique for ocean modeling based on the smoothed semi-prognostic method. *Ocean Dynam.* 55, 162–177. <https://doi.org/10.1007/s10236-005-0005-6>.
- Stelling, G.S., Wiersma, A.K., Willemse, J.B.T.M., 1986. Practical aspects of accurate tidal computations. *J. Hydraul. Eng.* 112, 802–816.
- Taeb, P., Weaver, R.J., 2017. Automated multi-grid tool for high resolution estuarine modeling. In: ADCIRC Users Group Meeting. Boston.
- Tezduyar, T., Aliabadi, S., Behr, M., Johnson, A., Kalro, V., Litke, M., 1996. Flow simulation and high performance computing. *Comput. Mech.* 18, 397–412.
- Walters, R.A., Carey, G.F., 1983. Analysis of spurious oscillation modes for the shallow water and Navier-Stokes equations. *Comput. Fluids* 11, 51–68. [https://doi.org/10.1016/0045-7930\(83\)90013-0](https://doi.org/10.1016/0045-7930(83)90013-0).
- Weaver, R.J., Slinn, D.N., 2005. Effect of wave forcing on storm surge. In: *Coastal Engineering* (2004), pp. 1532–1538.
- Westerink, B.J.J., Luettich, R.A., Scheffner, N.W., 1992. Tide and storm surge predictions using finite element model. *Hydraul. Eng.* 118, 1373–1390.
- Westerink, J.J., Luettich, R.A., Feyen, J.C., Atkinson, J.H., Dawson, C., Roberts, H.J., Powell, M.D., Dunion, J.P., Kubatko, E.J., Pourtaheri, H., 2008. A basin- to channel-scale unstructured grid hurricane storm surge model applied to southern Louisiana. *Mon. Weather Rev.* 136, 833–864. <https://doi.org/10.1175/2007MWR1946.1>.
- Zheng, L., Weisberg, R.H., 2012. Modeling the west Florida coastal ocean by downscaling from the deep ocean , across the continental shelf and into the estuaries. *Ocean Model.* 48, 10–29. <https://doi.org/10.1016/j.ocemod.2012.02.002>.